University of Groningen

The organic ties of iron

Slagter, Hans Arent

IMPORTANT NOTE: You are advised to consult the publisher's version (publisher's PDF) if you wish to cite from it. Please check the document version below.

Document Version
Publisher's PDF, also known as Version of record

Publication date:
2018

[Link to publication in University of Groningen/UMCG research database](#)

Citation for published version (APA):
Slagter, H. A. (2018). *The organic ties of iron: Or the origin and fate of Fe-binding organic ligands*. [Thesis fully internal (DIV), University of Groningen]. Rijksuniversiteit Groningen.

Chapter 6

Fe-binding Organic Ligands in the Humic-Rich TransPolar Drift in the Surface Arctic Ocean using Multiple Voltammetric Methods

Abstract

Samples inside and outside of the Arctic Ocean's transpolar drift (TPD) have been analysed for Fe-binding organic ligands with Competitive Ligand Exchange Adsorptive Stripping Voltammetry (CLE-AdCSV) using salicylaldoxime (SA). This analysis is compared to prior analysis with CLE-AdCSV using 2-(2-thiazolylazo)-p-cresol (TAC). The TPD's strong terrestrial influence is used to compare the performance of both CLE-AdCSV methods in representing the nature of the natural organic ligands. These measurements are compared against direct voltammetric determination of humic substances (HS) and spectral properties of dissolved organic matter. The relations between the two CLE-AdCSV derived organic ligand concentrations and HS in the TPD have a comparable slope, though with an offset of 40% towards higher values for the SA method. These higher organic ligand concentrations, most probably due to HS, explain the high dissolved Fe concentrations transported over the Arctic Ocean by the TPD.

Outside the core of the TPD in the surface Arctic Ocean HS occur as well but at lower concentrations. Here HS still relate to dissolved Fe concentrations and to organic ligand concentrations obtained with SA, whereas organic ligand concentrations obtained with TAC remain constant. Moreover with decreasing HS the offset between the methods using TAC and SA decrease to smaller values. We hypothesize that the method using TAC either detects HS only at higher concentrations or detects only HS of a specific composition. On the other hand, the SA method might overestimate organic ligand concentrations as the offset with the TAC method remains where HS are not detected.

Ultimately, multiple approaches will be required to elucidate origin and nature of Fe-binding organic ligands in the marine environment.

6.1. Introduction

Fe is an essential trace metal for marine primary production (Geider and La Roche, 1994; Netz et al., 2012; Zhang, 2014). Fe solubility in seawater is governed by the presence of organic ligands to bind Fe, as inorganic solubility is lower than the minimum required concentrations for primary productivity (Timmermans et al., 2001a, 2001b; Strzepek et al., 2011; Boyd et al., 2012; Wilhelm et al., 2013). Fe-binding organic ligands form a poorly characterized pool as part of Dissolved Organic Matter (DOM; Gledhill and Buck, 2012; Hassler et al., 2017). Some very specific contributors such as siderophores are now becoming better characterized, though the relative contribution of these is in picomolar ranges and are a minor fraction of DFe and the Fe-binding organic ligand concentrations (Gledhill et al., 2004; Velasquez et al., 2011, 2016; Boiteau et al., 2016; Bundy et al., 2018). Given the inherently indirect nature of Fe-binding organic ligand measurements, the relative contribution of different groups of Fe-binding organic ligands is as of yet unknown. However, relative contributions by groups like humic substances (HS; Laglera and van den Berg, 2009) and exopolymeric substances (EPS; Hassler et al., 2011) may be considerable, given that there is no single contributor to the ligand pool indicated that explains Fe-binding ligand concentrations up to the nanomolar range as of yet.

The surface of the Arctic Ocean is strongly affected by terrestrial DOM as it is a shelf-surrounded ocean subject to terrestrial influences with a very high source area to basin ratio as defined by Raiswell and Anderson (2005). Runoff from the many rivers contains complex organic material, which for a large part is deposited in the Arctic shelf seas. The input of terrestrial HS is thought to be a major influence in the context of Fe-binding organic ligands. HS are persistent and heterogenic complex organic degradation products, ubiquitous particularly in coastal areas (Buffle, 1990) and long known to bind trace metals (Buffle, 1988). In fact, HS have been shown to account for an important part of the Fe-binding capacity in seawater (Laglera and van den Berg, 2009; Abualhaija et al., 2015; Dulaquais et al., 2018). HS are a complex black box with components that are typically operationally defined. Humic acids are hydrophobic at low pH and therefore separated from fulvic acid by precipitation after acidification (Buffle, 1988; Bronk, 2002), these form the oldest or most recalcitrant fraction of HS. A distinction is also made between terrestrial HS and marine humic or humic-like substances, produced in-situ by marine microbial activity as opposed to transported in from a terrestrial source (Bronk, 2002; Nakayama et al., 2011). However, this distinction is hypothetical and cannot be supported by analytical means. Low salinity waters in the surface Arctic Ocean carry important

DOM concentrations of terrestrial nature whereas marine humics could contribute significantly to higher salinity waters.

Here we study a selection of samples from the ice covered Arctic Ocean and one of the open shelf seas. The surface of the Arctic Ocean is of particular interest due to the relatively well-constrained Transpolar Drift (TPD) surface current. It is well established that the TPD transports riverine-based water and ice from the shelf seas across the Arctic Ocean, eventually out to the Atlantic Ocean through the Fram Strait (Gordienko and Laktionov, 1969; Gregor et al., 1998). The flow path of the TPD varies yearly with the arctic oscillation index (Macdonald et al., 2005) and has been constrained in the context of DOM and Fe biogeochemistry (Rijkenberg et al., 2018, Chapter 4; Slagter et al., 2017, Chapter 5). Given its susceptibility to rapid climate change (IPCC, 2014), the Arctic Ocean is a particularly important region to study the biogeochemistry of terrestrial matter. Rapid and widespread loss of permafrost (Schuur et al., 2015) in the river catchments is indicated to cause increases in the deposition of terrestrial organic matter in the Arctic shelf seas (Vonk et al., 2013) and effects on the larger Arctic Ocean are as of yet largely unknown. In the present study samples were collected during the 2015 PS94 TransArcII expedition inside the TPD and therefore subject to the terrestrial influence from major Arctic rivers; outside the TPD and in the Barents Sea, majorly under influence of the shelf and Atlantic inflow (Rudels, 2012). Early *in-situ* measurements of HS and CDOM establish that the TPD carries HS, though they were also detected in nontrivial concentrations outside of the TPD flow path (Chapter 5), which is unsurprising as HS and/or marine humics are ubiquitous also in non-coastal waters (Obernosterer and Herndl, 2000).

The definition of HS is essentially operational based on column retention with alkaline elution (Buffle, 1990). These analytical techniques are very time consuming and hard to apply in seawater. Spectral properties of DOM (Chromophoric DOM or CDOM and Fluorescent DOM or FDOM) are indicative of many subgroups, including HS (Coble, 2007). Measurements of HS and their relative contribution to the Fe-binding organic ligand pool are not straightforward. Direct voltammetric measurement of HS is possible, with HS indicated by standard addition of a representative reference material (Laglera et al., 2007; Quentel and Filella, 2008; Laglera and van den Berg, 2009).

Measurement of Fe-binding organic ligands using Competitive Ligand Exchange – Adsorptive Cathodic Stripping Voltammetry (CLE-AdCSV) is a technique proven to resolve the presence of most major ligands in the ocean (Gledhill and van den Berg, 1994; Rue and Bruland, 1995; Croot and Johansson, 2000; van den Berg, 2006). However, elucidation of the contribution of HS meets with mixed results. Voltammetric determination of Fe-binding organic ligands

measures the concentration and binding strength integrally for the Fe-binding organic ligand pool as a whole, and these are at best divided into several groups by binding strength. The method using 2-(2-thiazolylazo)-p-cresol (TAC) as a competing ligand (Croot and Johansson, 2000) has been shown not to reflect humic influences (Laglera et al., 2011). In contrast, recent work using salicylaldoxime (SA) as competing ligand has been shown to indicate HS (Laglera et al., 2011; Abualhaija and van den Berg, 2014; Mahmood et al., 2015).

In Chapter 5 we reported a strong relation between Fe-binding organic ligand measurements using TAC and the presence of the TPD as well as humic representative CDOM and FDOM measurements. The present study expands on this by re-analysing select samples from that study using SA as a competing ligand in CLE-AdCSV and additional measurements of HS. Comparing these results with those of TAC we provide an explanation to the values of ligand concentration below dissolved iron concentrations found in Chapter 5 and hope to further unveil the relative contribution of HS in the Fe-binding organic ligand pool in the Arctic Ocean in the TPD and in the coastal Barents Sea.

6.2. Materials and Methods

Specific samples collected during the 2015 PS94 TransArcII expedition on board FS Polarstern were analysed during the cruise with the TAC method (Chapter 5) and a subset of samples stored at -20 °C and re-analysed using CLE-AdCSV with SA. Re-analysis of samples with the SA method was performed for stations 69, 99, 101, 125 and 153 (Figure 1). Stations 69 and 125 are full depth profiles in the open Arctic Ocean (3500 and 4200 m, respectively); station 153 is a full depth profile over the Barents Sea shelf (400 m); and stations 99 and 101 have been sampled for the top 200 m. The SA method of analysis was applied according to Rue and Bruland (1995) following the adaptations by Buck et al. (2015).

A subset of frozen samples was analysed after cruise in the laboratories of the University of the Balearic Islands (UIB lab) with a voltammetric system identical to the system used on board. In this case the original voltammetric method (Laglera et al., 2007) was slightly modified to ensure the saturation with iron of the HS binding groups of both the sample and the reference standard (Sukekava et al., 2018). In the presence of 20 nM $KBrO_3$ and 5 mM POPSO buffer (from a mixed solution cleaned with MnO_2 as in Laglera et al., 2013) the sample was saturated with iron (20-60 nM depending on the DFe concentration) and was continually measured until the voltammetric signal decreased to a constant value. This decrease is caused by the total precipitation of iron in excess of the binding capacity of the HS. This process was described in Laglera and van den

Berg (2009). Calibration was attained via additions of 0.2 mg SRFA L^{-1}, dissolved in ultrapure water and in this case carefully saturated with iron before use. HS were therefore expressed as mg SRFA L^{-1}. The datasets for [HS] from both labs (on board and UIB lab) showed good correlation and could therefore safely be combined into one (Sukekava et al., 2018), and are from here on reported after conversion to $[L_t]_{FA}$ for most purposes. A complexing capacity of 14.6±0.7 mg SRFA L^{-1} (Sukekava et al., 2018). was used to convert HS concentrations into HS derived ligand concentrations ($[L_t]_{HS}$).The complexing capacity was obtained by titration with iron of the SRFA standard dissolved in UV digested seawater as suggested in Laglera and van den Berg (2009).
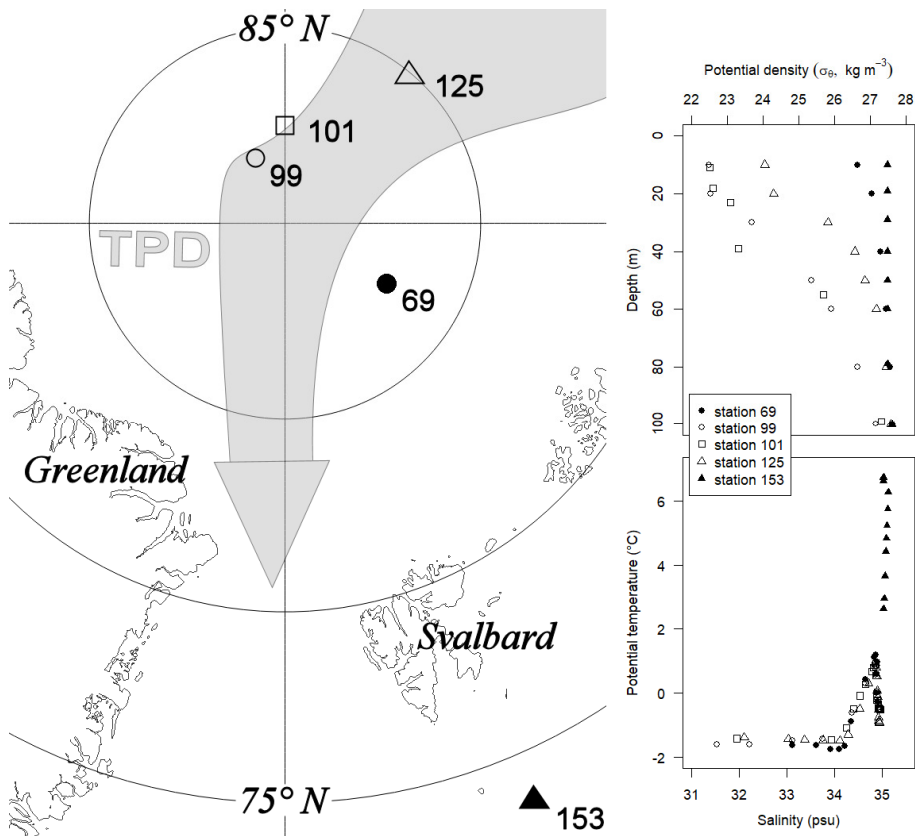

Figure 1 Map of the study area showing the selected stations 69, 99, 101, 125 and 153. The expected flow path of the TPD after Slagter et al. (2017, Chapter 5) is shown by the grey arrow. Potential density (top right) is shown for the upper 100 m indicating the TPD influence. A potential temperature-salinity (Θ-S) plot of the selected stations is shown to the lower right.

6.3. Results

6.3.1. Overall oceanographic characteristics

The TPD influence area in the Arctic Ocean surface coincides with a low density anomaly resulting from low surface salinity within the upper 100 m. Specifically, surface samples from Stations 99, 101 and 125 inside the TPD, as defined in Chapter 5 by in-situ CDOM fluorescence ≥ 0.5 a.u. (Rabe et al., 2016), show this low surface salinity and density (Figure 1, open symbols), down to 28 psu and 23 kg m^{-3}, respectively. Station 69, outside the TPD, has a higher surface salinity and density of 33.5 psu and 27 kg m^{-3}, respectively. Station 153 in the Barents Sea has a salinity of >35 psu and relatively constant density between 27.5 and 28 kg m^{-3} with a higher potential temperature (3-7 °C, Figure 1). From the three stations in the TPD, station 101 is bordering closely rather than inside.

6.3.2. Arctic Fe speciation

All SA measurements show higher [L_t] than the TAC measurements (Figure 2 second row vs. first row, Excess L in Figure 3B). Specifically, [L_t]$_{TAC}$ is an average 60% of [L_t]$_{SA}$ across all samples that have data for both methods(SD = 12.9%, N = 47). At depths beyond 150 m [L_t]$_{SA}$ approaches the [L_t]$_{TAC}$ more closely. The difference is most pronounced for measurements inside the TPD. [L_t]$_{TAC}$ inside the TPD was in some cases lower than DFe (Stations 99 and 125, Figure 2, top row), with more occurrences in the complete TAC dataset (Chapter 5). This was not the case for [L_t]$_{SA}$, which was higher than DFe in all samples measured. Overall, [L_t]$_{TAC}$ was 2.46±0.63 Eq. nM Fe inside the TPD and 1.36±0.33 eq. nM Fe outside the TPD; [L_t]$_{SA}$ was 4.19±0.74 and 2.33±0.58 Eq. nM Fe, respectively (Table 1). In contrast to TAC data, most SA analyses could also be resolved for 2 ligand groups inside the TPD. When comparing the sum of SA-derived [L_1] and [L_2] from the 2 ligand model ($\Sigma_{L1,L2;SA}$) to [L_t]$_{SA}$ from the model assuming the existence of 1 ligand, there is very good agreement (Figure 2, second row). Additionally, the SA-derived [L_1] has a good agreement with [L_t]$_{TAC}$ (Pearson's product-moment correlation score of 0.82 (p<0.001; N=12). For those samples where 2 ligand groups could be resolved for the TAC method, $\Sigma_{L1,L2;TAC}$ is higher than [L_t]$_{TAC}$. High surface [L_t]$_{HS}$ (Figure 2, bottom row) was especially pronounced in the two unequivocal TPD stations (99 and 125) with [L_t]$_{HS}$ over 4 Eq. nM Fe in the upper 50 m, coinciding with high values of parameters describing CDOM. [L_t]$_{HS}$ was elevated to a lesser extent in the surface in the TPD-bordering station 101 and station 69 outside the TPD, and no elevated concentrations were observed for station 153 in the Barents Sea. The difference between measurements of [L_t] using TAC and SA ([L_t]$_{SA}$ - [L_t]$_{TAC}$) are referred to as δLt. δLt was consistently >0 with a value inside the TPD of 1.73±0.56 Eq. nM Fe whereas outside the TPD and over the continental shelf

outside the TPD flow path δLt is lower, but still considerable at 0.92±0.44 and 0.81±0.43 Eq. nM Fe, (Table 1, ranges given are standard deviations).

LogK´$_{Fe´L}$ is similar for either method and remarkably stable (table 1). Measurements using TAC have a logK´$_{Fe´L}$ of 12.01±0.39 mol^{-1} inside the TPD, and 12.13±0.23 mol^{-1} outside the TPD. Measurements using SA have a logK´$_{Fe´L}$ of 11.75±0.35 mol^{-1} inside the TPD and 11.60±0.27 mol^{-1} outside the TPD. In the Barents Sea logK´$_{Fe´L}$ using TAC is similar to the other subsets at 12.14±0.17 mol^{-1}, whereas here the SA method results in a lower logK´$_{Fe´L}$ of 11.17±0.20 mol^{-1} which has very little SD overlap. Figure 3 shows the relation between the TAC and SA methods in terms of log$\alpha_{Fe´L}$, and excess L. Log$\alpha_{Fe´L}$ is less prone to bias and therefore a good parameter for comparison (Gledhill and Gerringa, 2017). For the SA method log$\alpha_{Fe´L}$ is invariably near 3, for the TAC method log$\alpha_{Fe´L}$ is near 3 outside the TPD, inside the TPD values decrease to below 1 (Table 1, Figure 3A). Since logK´$_{Fe´L}$ does not significantly change inside the TPD, the low log$\alpha_{Fe´L}$ values for the TAC method are tied to the excess ligand concentration. Saturation of the measured ligands is indicated with excess ligands near zero and thus logK´$_{Fe´L}$ values that are difficult to calculate. This is caused by a lack of data points with large standard deviations, thus resulting in log$\alpha_{Fe´L}$ values that are imprecise (Gerringa et al., 2014). Measurements using the TAC method give consistently lower excess ligand concentrations for all depths, including sporadic occurrence of near-zero values (Figure 3B; Table 1).
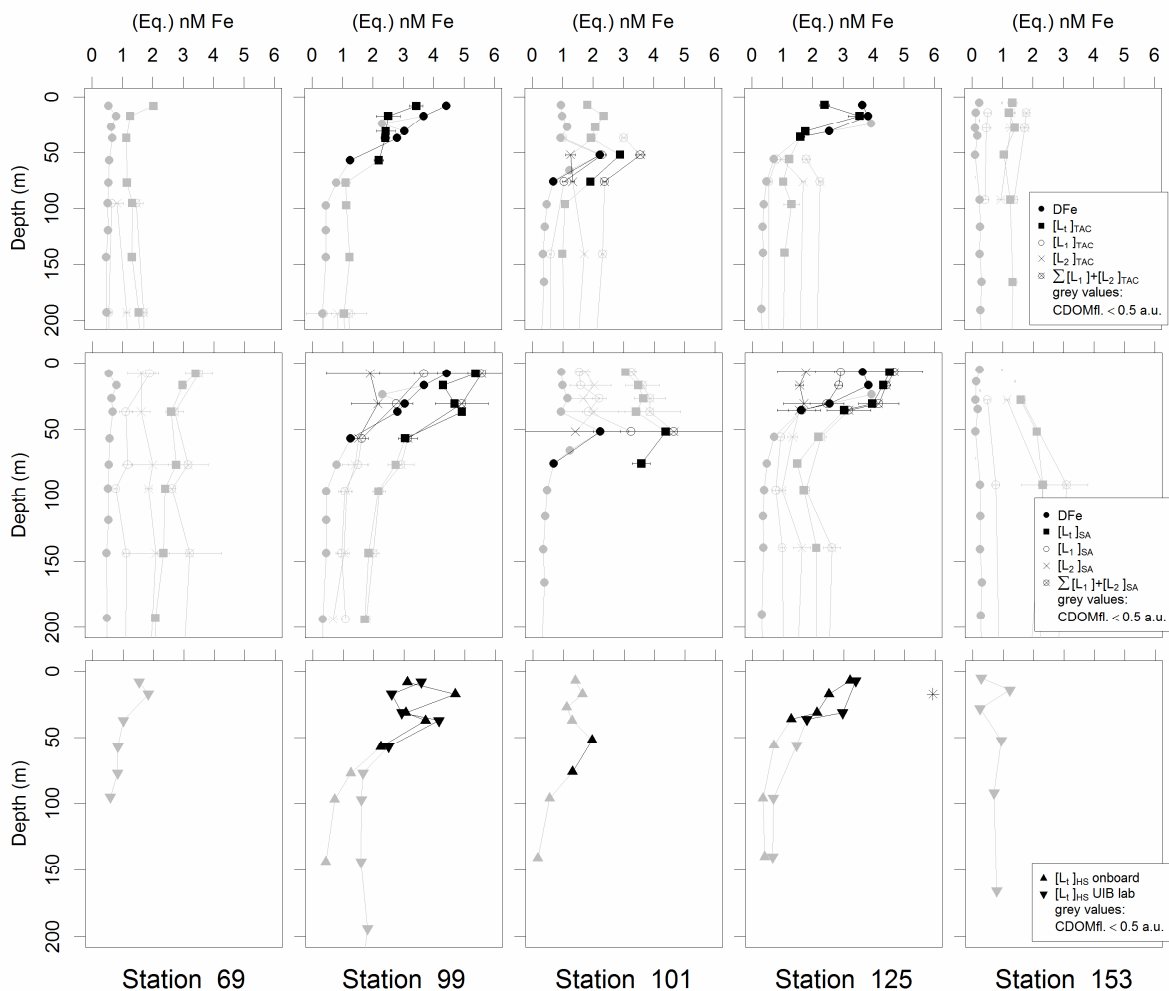
Figure 2 DFe and ligand concentrations for determinations using two models one allowing 1 ligand ($[L_t]$), and one allowing two ligands ($[L_1]$ and $[L_2]$) to exist. Per station results obtained using TAC are in the top row, and those using SA are in the middle row. The bottom row shows equivalent ligand concentrations derived from SRFA complexing capacity for HS measurements in two labs. Samples outside the TPD (grey symbols) and inside the TPD (black symbols) are determined by the CDOM fluorescence (CDOMfl.) ≤ 0.5 a.u. boundary for all graphs.

Figure 3 Log$\alpha_{Fe'L}$ (**A**, dimensionless) and Excess L (**B**, [L′] in Eq. nM Fe) for 1-ligand class determination by depth using TAC (closed circles) and SA (open squares). Samples outside the TPD (grey symbols) and inside the TPD (black symbols) are determined by the CDOMfl. ≤ 0.5 a.u. boundary for all graphs.

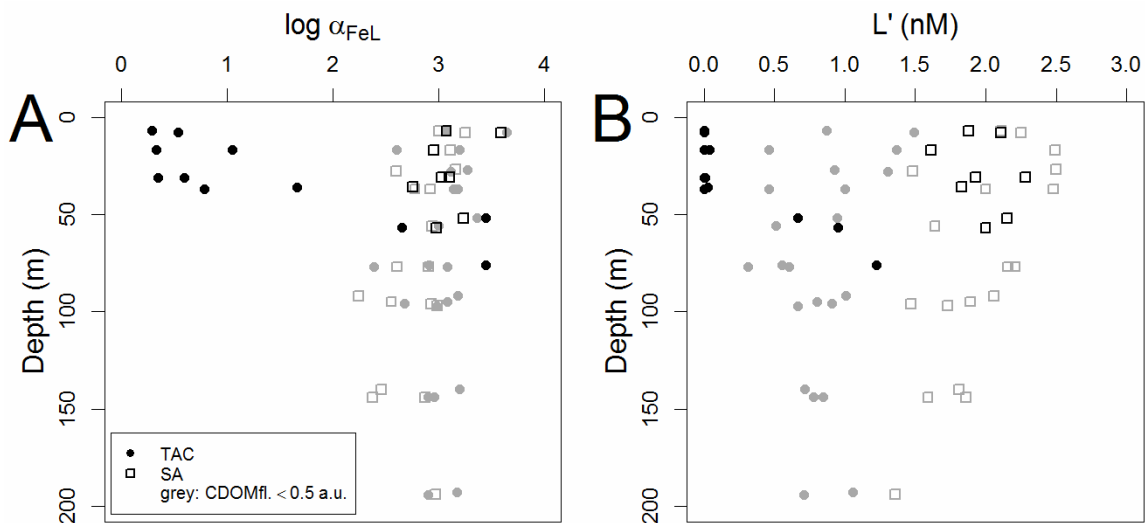**Table 1** DFe and Fe-binding organic ligand characteristics using a 1-ligand-class model for calculation using both the TAC and SA method of CLE-AdCSV for samples from stations 69–125 separated by TPD presence based on CDOMfl. $\leq$ 0.5 a.u. and for samples from station 153 in the Barents Sea separately. Properties include the ligand concentration [L_t] and the absolute difference in L_t between CLE-AdCSV methods (δL_t) as well as relative to [L_t]$_{SA}$; the relative complexation capacity attributed to HS determined directly through standard addition with SRFA ([L_t]$_{HS}$); the conditional binding constant relative to Fe′ (log$K'_{Fe'L}$), the excess ligand concentration (L′), and the reactivity relative to Fe′ (log$\alpha_{Fe'L}$).

		DFe	[L_t]$_{TAC}$	[L_t]$_{SA}$	δL_t	[L_t]$_{TAC}$ /[L_t]$_{SA}$	[L_t]$_{HS}$	log$K'_{Fe'L}$ (TAC)	log$K'_{Fe'L}$ (SA)	L′$_{TAC}$	L′$_{SA}$	log$\alpha_{Fe'L}$ (TAC)	log$\alpha_{Fe'L}$ (SA)
		nM	*Eq. nM Fe*			*%*	*Eq. nM Fe*	*mol⁻¹*	*mol⁻¹*	*Eq. nM Fe*			
Inside TPD	*mean*	2.70	2.46	4.19	1.73	59%	2.83	12.01	11.75	0.27	2.05	1.38	3.05
CDOMfl. ≥ 0.5 a.u.	*SD*	1.17	0.63	0.74	0.56	11%	0.97	0.39	0.35	0.46	0.40	1.24	0.33
St. 99, 101 and 125	*N*	11	11	11	11	11	11	11	11	11	11	11	11
	min	0.69	1.6	3.03	0.76	45%	1.3	11.45	10.89	0	1.41	0.29	2.35
	max	4.42	3.55	5.37	2.51	82%	4.22	12.63	12.27	1.23	2.88	3.45	3.59
Outside TPD	*mean*	0.50	1.36	2.33	0.92	62%	1.04	12.13	11.6	0.86	1.77	3.04	2.84
CDOMfl. < 0.5 a.u.	*SD*	0.22	0.33	0.58	0.44	13%	0.5	0.23	0.27	0.27	0.40	0.27	0.28
St. 69, 99, 101 and	*N*	44	44	44	32	32	19	44	32	44	32	44	32
125	*min*	0.15	0.89	1.48	0.13	41%	0.16	11.67	11.11	0.31	1.16	2.39	2.38
	max	1.15	2.36	3.65	1.71	93%	1.83	12.62	12.35	1.49	2.5	3.69	3.65
Barents Sea	*mean*	0.31	1.26	2.04	0.81	62%	0.70	12.14	11.17	0.95	1.67	3.07	2.38
Station 153	*SD*	0.31	0.12	0.31	0.43	18%	0.38	0.16	0.20	0.34	0.44	0.24	0.18
	N	7	7	4	4	4	6	7	4	7	4	7	4
	min	0.11	1.05	1.59	0.18	50%	0.24	11.95	10.93	0.23	1.15	2.61	2.23
	max	0.98	1.41	2.32	1.07	89%	1.22	12.39	11.43	1.31	2.06	3.37	2.6

While 2 ligand groups could be resolved for few of the TAC-derived measurements, especially in the surface, yielding few records for comparison, the $LogK'_{Fe'L}$ values for the L_1 class agree well for the TAC and SA methods (Figure S1, second column of graphs). This agreement is dependent on α_i, as using $LogK'_{FeL,Fe3+}$ results in better agreement for the L_2 class (data not shown). Such correlations based on $logK'_{FeL,Fe3+}$ are an artefact of the pH used in analysis through α_i. As our TAC measurements are performed at pH=8.05 and our SA measurements are performed at pH=8.40, $logK'_{FeL,Fe3+}$ is not a suitable comparison (Gledhill and Buck, 2012). Over the entire dataset $logK_1'_{Fe'L(SA)}$ and $logK_1'_{Fe'L(TAC)}$ do not differ significantly, with values of 13.88±0.65 (N = 41) and 13.49±0.58 mol^{-1} (N = 26) respectively. The weaker L_2 class is found to be significantly stronger in the case of TAC measurements, with an average $logK_2'_{Fe'L,(SA)}$ of 10.43±0.21 mol^{-1} and an average $logK_2'_{Fe'L(TAC)}$ of 11.19±0.21 mol^{-1}. This difference in particular would have been veiled had K' been reported in relation to Fe^{3+} here, since the difference between the values is ~0.8. $Log\alpha_{Fe'L}$ (Figure S1, third column, page 138) is higher towards the surface for the SA-derived L_1 fraction. Over the Barents Sea shelf (station 153), values are very similar regardless of the CLE-AdCSV method employed.

6.3.3. Method intercomparison

When comparing $[L_t]$ between the TAC and SA methods directly, the initial view is a reasonable agreement with consistently higher values for $[L_t]_{SA}$ as noted in the prior paragraphs. All points are below the 1:1 line in favour of $[L_t]_{SA}$ (Figure 4). When we separate the data using CDOMfl. ≤ 0.5 a.u. boundary, dividing samples inside and outside the TPD, the CLE-AdCSV methods show distinct relations with one outlier, the uppermost sample of station 69 (10 m depth; triangle in Figure 4). The relationship between $[L_t]_{TAC}$ and $[L_t]_{SA}$ at station 101 indicates that this station is in the TPD influence zone (crosses in Figure 4). Samples inside the TPD correlate with a slope of 0.56 ($[L_t]_{TAC}$:$[L_t]_{SA}$), whereas outside the TPD there is no correlation, with $[L_t]_{TAC}$ unchanging while $[L_t]_{SA}$ varies between samples.

$LogK'_{Fe'L}$ for the measurements using SA were lower than those for the measurements using TAC, but otherwise shared in a remarkable consistency observed earlier for this dataset (Chapter 5). The only exception herein is the Barents Sea station, where the difference between TAC- and SA-derived $logK'_{Fe'L}$ was slightly higher due to lower $logK'_{Fe'L}$ for measurements using SA. $Log\alpha_{Fe'L}$ for the SA analyses does not significantly differ inside and outside the TPD. In contrast, $log\alpha_{Fe'L}$ for TAC analyses is significantly lower inside the TPD.

Increments in DFe, $[L_t]_{TAC}$ and $[L_t]_{SA}$ crossing into the TPD influence were compared to increments in [HS] based on the same boundary. Resulting is an

increment ratio between ΔDFe, $\Delta[L_t]_{TAC}$ and $\Delta[L_t]_{SA}$ over $\Delta[HS]$ (Table 2). For instance, the increment ratio for DFe may be defined as:

$$\frac{\Delta DFe}{\Delta[HS]} = \frac{\overline{DFe_{inside\,TPD}} - \overline{DFe_{outside\,TPD}}}{[HS]_{inside\,TPD} - [HS]_{outside\,TPD}} \quad\quad (1)$$

The $\Delta[L_t]/\Delta[HS]$ ratio is lower for TAC measurements than for SA measurements, 8.4 Eq. nM Fe mg^{-1} and 12.2 Eq nM Fe mg^{-1}, respectively. The $\Delta DFe/\Delta[HS]$ ratio is higher at 17.4 nM mg^{-1}. The lower ratio $\Delta[L_t]_{TAC}/\Delta[HS]$ indicates a lack of representation of $\Delta[HS]$ in $[L_t]_{TAC}$. However, as it is 68% of $\Delta[L_t]_{SA}/\Delta[HS]$ as opposed to near-zero, some contribution to [HS] is detected by TAC. The $\Delta DFe/\Delta[HS]$ and $\Delta[L_t]_{SA}/\Delta[HS]$ ratios resemble more the binding capacity of 14.6±0.7 nM mg^{-1} found for the SRFA standard and the value of 16.7 nM mg^{-1} as found by Laglera and van den Berg (2009).
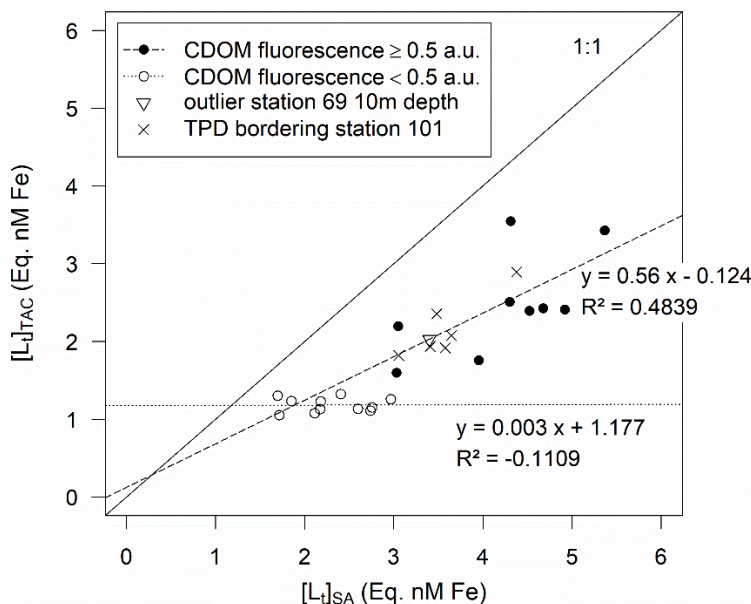
Figure 4 The ligand concentrations $[L_t]$ in Eq. nM Fe as measured using CLE-AdCSV with TAC (vertical) and SA (horizontal), samples are subdivided on the basis of their presence inside the TPD (filled symbols, CDOMfl. ≥ 0.5 a.u.) and outside the TPD (open symbols, CDOMfl. < 0.5 a.u.). One value does not conform to the split (triangle symbol), which is objectively outside the TPD influence area, this value is not included in the regressions. Functions and R^2 values describe the linear regressions of the subsets inside and outside the TPD. Station 101, indicated by crosses, is considered inside the TPD.

Table 2   Average concentrations with standard deviations of DFe, $[L_t]$ (using two CLE-AdCSV methods) and [HS] inside and outside the TPD based on CDOM fluorescence. The increments (Δ) across the CDOM fluorescence boundary (0.5 a.u.) of the averages are calculated for each property, and increments divided by Δ[HS] for DFe and $[L_t]$ per mg SRFA across the TPD border.

	DFe	**$[L_t]_{TAC}$**	**$[L_t]_{SA}$**	**[HS]**
	nM	*Eq. nM Fe*	*Eq. nM Fe*	*Eq. mg L^{-1}*
inside TPD	2.70±1.17	2.46±0.63	4.19±0.73	0.18±0.07
outside TPD	0.50±0.22	1.40±0.42	2.64±0.65	0.05±0.03
Δ (increment)	**2.20**	**1.06**	**1.55**	**0.13**
$\Delta[HS]^{-1}$	**17.4**	**8.4**	**12.2**	**1**

The $[L_t]_{HS}$ and DFe have a distinct relation inside the TPD, near the 1:1 line (Figure 5A). Comparing $[L_t]_{HS}$ to TAC- and SA-derived $[L_t]$ inside the TPD (Figure 5B), both relate almost similarly though with an offset between the two comparisons (intercepts of -0.40 and 0.88 Eq. nM Fe for linear regressions of $[L_t]_{TAC}$:$[L_t]_{HS}$ and $[L_t]_{SA}$:$[L_t]_{HS}$ in Figure 5B, respectively). While $[L_t]_{TAC}$ correlates with $[L_t]_{HS}$ in a near 1:1 ratio (slope is 0.99), $[L_t]_{SA}$ has a consistently higher value while maintaining a smaller slope (0.89). Outside the TPD $[L_t]_{TAC}$ is constant over low but variable $[L_t]_{HS}$, whereas $[L_t]_{SA}$ and $[L_t]_{HS}$ outside the TPD co-vary similarly to their relation inside the TPD (grey values in Figure 5B). The lack of $[L_t]_{TAC}$ correlation with $[L_t]_{HS}$ outside the TPD corresponds to a poorer correlation of $[L_t]_{HS}$ with DFe outside of the TPD (Figure 5A). Comparison between $[L_t]_{HS}$ and δL_t shows no clear correlation inside and outside of the TPD,. Pearson product-moment correlation proved to be highly significant for $[L_t]_{HS}$ with DFe, with the strongest r values for samples inside the TPD. Similar relations between r values are seen for $[L_t]_{HS}$ vs. $[L_t]_{SA}$ and $[L_t]_{TAC}$, though with lower significance levels and no formal significance for the latter for samples outside of the TPD (Table 3). In contrast, the relation between $[L_t]_{HS}$ and δL_t was only significant for samples outside of the TPD, though there is a relation closer to a 1:1 ratio for the entire dataset (Table 3, Figure 5C). Paradoxically to the ratios of increment above and the occurrence of ligand saturation for measurements using TAC, the correlation score for the $[L_t]_{HS}$-$[L_t]_{TAC}$ relation inside the TPD is very similar to the $[L_t]_{HS}$-$[L_t]_{SA}$ relation.
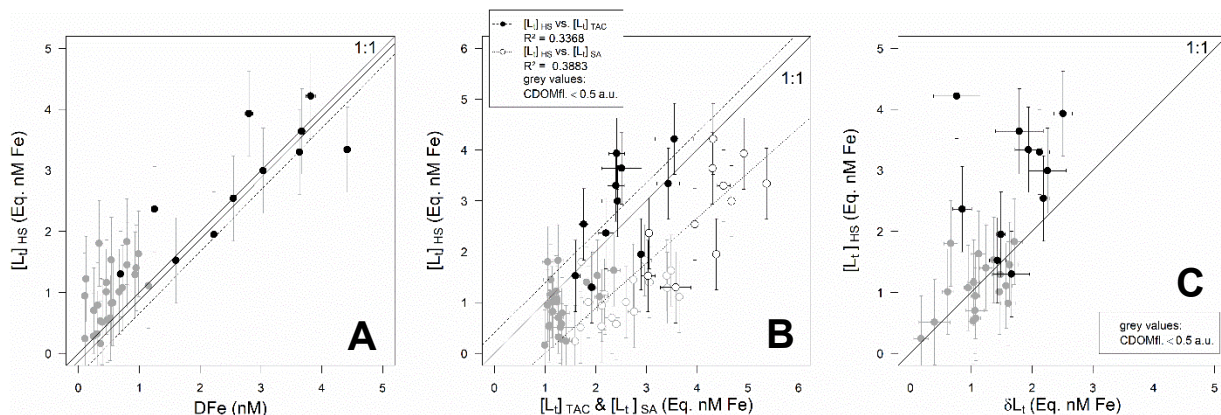
Figure 5 **A**) Comparison of $[L_t]_{HS}$ and DFe. The error bars along the vertical axis are derived from the uncertainty of 0.7 nM mg^{-1} in the conversion factor from [HS] to $[L_t]_{HS}$. R^2 values indicate the quality of fit of linear regressions, of which those for all data and data inside the TPD (CDOMfl. ≥ 0.5 a.u.) are plotted. **B**) Comparison of $[L_t]_{HS}$ with $[L_t]$ derived from CLE-AdCSV with SA (open symbols) and TAC (closed symbols). Only measurements inside the TPD (CDOMfl. ≥ 0.5 a.u.) were considered for the linear regressions. **C**) Comparison of $[L_t]_{HS}$ with the difference between CLE-AdCSV-derived $[L_t]$ values (δL_t) inside the TPD (black) and outside the TPD (grey). Grey values represent values outside of the TPD (CDOMfl. < 0.5 a.u.).

Table 3 Pearson product-moment correlation scores (r) for relations between $[L_t]_{HS}$ and DFe, $[L_t]$ by two CLE-AdCSV methods. Correlation significance levels are p<0.005***, p<0.01** and p<0.05*. Lower- and upper limits of 95% confidence intervals for correlations scores are reported in the last two columns.

relation	r	p-value		95% conf. LL	95% conf. UL
$[L_t]_{HS}$ vs. DFe inside TPD	**0.83**	**0.001**	*******	**0.46**	**0.96**
$[L_t]_{HS}$ vs. DFe outside TPD	**0.55**	**0.004**	*******	**0.20**	**0.78**
$[L_t]_{HS}$ vs. $[L_t]_{TAC}$ inside TPD	0.63	0.036	*	0.06	0.89
$[L_t]_{HS}$ vs. $[L_t]_{TAC}$ outside TPD	0.38	0.063		0	0.67
$[L_t]_{HS}$ vs. $[L_t]_{SA}$ inside TPD	0.67	0.024	*	0.12	0.91
$[L_t]_{HS}$ vs. $[L_t]_{SA}$ outside TPD	0.52	0.022	*	0.09	0.79
$[L_t]_{HS}$ vs. δL_t inside TPD	0.17	>> 0.05		0	0.70
$[L_t]_{HS}$ vs. δL_t outside TPD	0.49	0.031	*	0.05	0.77

6.4. Discussion

6.4.1. Arctic Fe speciation

Stations inside the TPD influence area show an increase in DFe and Fe-binding organic ligands along with HS representative properties such as [HS] and CDOM fluorescence. When measured using the TAC method these higher concentrations have been found to correlate significantly to known descriptors of riverine influences and HS in particular (Chapter 5). At stations 99 and 125 the $[L_t]_{TAC}$ was lower than DFe for 4 and 3 samples inside the TPD, respectively (Figure 2), suggesting that there are insufficient ligands to bind Fe and thus explain DFe. In contrast, $[L_t]_{SA}$ is higher than DFe in all samples, explaining the high Fe solubility in the TPD. The good correlation between HS and DFe indicates that HS is responsible for this high solubility.

The difference between $[L_t]_{TAC}$ and $[L_t]_{SA}$ is more pronounced inside the TPD but still present outside the TPD. There is a remarkably similar LogK'$_{Fe'L}$ inside and outside of the TPD. Mahmood et al. (2015) found an average range of $10.60 \leq logK´_{Fe´L} \leq 12.74$ mol^{-1} and a correlation between $[L_t]$ and HS in the Liverpool Bay area (Irish Sea). Abualhaija et al. (2015) found similar values in the same area ($11.1 \leq logK'_{Fe'L} \leq 11.3$ mol^{-1}). Measurements by Batchelli et al. (2010) in the Thurso Bay area (Atlantic Ocean) put logK´$_{Fe´L}$ between 11.8 and 12.0 mol^{-1} whereas the dataset used for the Mediterranean HS by Gerringa et al. (2017) gave $11.57 \leq logK´_{Fe´L} \leq 12.13$ mol^{-1}. In the present study logK´$_{Fe´L}$ values fell within those found in the quoted studies, but lacking a significant difference between samples inside and outside the TPD (Table 1), whereas the differences in $[L_t]$ and [HS] were profound.

The TAC-derived logK'$_{Fe'L}$ in the Barents Sea was the same as the samples in the open Arctic Ocean. In contrast, the SA-derived logK'$_{Fe'L}$ was lower in the Barents Sea than in the open Arctic Ocean stations and the only significantly lower logK'$_{Fe'L}$ in comparison to TAC.

Results for 2 ligand classes where these could be resolved, closest to the surface primarily from measurements using SA (Figure S1), show two distinct classes based on K´, with across methods a strong L_1 class ranging $12.56 \leq logK´_{Fe´L} \leq 14.53$ mol^{-1} taking standard deviations into account, and a weaker L_2 class ranging $10.22 \leq logK´_{Fe´L} \leq 11.37$ mol^{-1}. Generally, there is a maximum spread of 1 to 2 orders of magnitude of $\alpha_{Fe´L}$ each side of D_{AL} considered to be an acceptable spread for CLE-AdCSV measurements (Apte et al., 1988; van den Berg et al., 1990; Gerringa et al., 2014). Between L_1 and L_2 for measurements using SA, this range is close to 4 orders of magnitude, though this is something that is not unique to the present study (Gledhill and Buck, 2012). In the present

study, the upper end of the $\log K'_{Fe'L}$ interval for the L_1 class may be outside of the detection window of SA and thus the large K' range may potentially be an artefact. The above ranges for L_2 have been connected to estuarine outflow and HS (Gledhill and Buck, 2012; Bundy et al., 2015). $\Sigma_{L1,L2;SA}$ agreed very well with $[L_t]_{SA}$. Therefore, the concentrations of Fe-binding organic ligands are probably good, but K' may be imprecise. Moreover, due to the formation of $FeSA_2$ which is not electroactive (Abualhaija and van den Berg, 2014) the sensitivity was low at low Fe concentrations making higher K' values more difficult to determine. In the few surface samples where 2 ligand groups could be resolved using TAC, K' is inside the detection window. There was a marked difference between $\Sigma_{L1,L2;TAC}$ and $[L_t]_{TAC}$, with the sum of the separate ligand groups being higher (Figure 2, top row). $\Sigma_{L1,L2;TAC}$ may explain the presence of the high DFe in the uppermost samples where these concentrations are not explained by $[L_t]_{TAC}$. However, the disagreement between $[L_t]_{TAC}$ and $\Sigma_{L1,L2;TAC}$ also indicates a troublesome fit of the 2-ligand Langmuir model, hampering data quality in this respect. Ostensibly, there is an issue measuring HS using TAC, as oversaturation of ligands is not likely to persist if it occurs and L_t and $\Sigma_{L1,L2}$ need to agree. These issues do not occur for measurements using SA. TAC not reflecting all HS is the most probable explanation, as revisited in the next section.

6.4.2. Method intercomparison

Overall $[L_t]_{TAC}$ and $[L_t]_{SA}$, while both reflecting increased Fe-binding organic ligands in the TPD, are fairly different to each other. With the conversion factor of 14.6 ± 0.7 nM mg^{-1} for [HS], allowing expression of Eq. nM Fe mg^{-1} (Sukekava et al., 2018), we add $[L_t]_{FA}$ as a third measure of Fe-binding organic ligands. However, we must remember that these are methodically constrained to be Fe-binding fulvic acids in practice. In comparing the ratios of DFe and $[L_t]$ over [HS], as well as the ratios of increment going into the TPD (Table 2, Figure 5), we find reasonable agreement with the above conversion factor in accounting for the presence of Fe in the Arctic Ocean. The conversion factor is lower than the [DFe]/[HS] increment ratio of 17.4 nM mg^{-1} (Table 2), and close to the 16.7 nM mg^{-1} as estimated by Laglera and van den Berg (2009).

The increment ratio of 12.2 for $[L_t]_{SA}$ (Table 2) is near the complexing capacity of 14.6 ± 0.7 nM mg^{-1} found for the SRFA standard and the DFe/HS ratio of 13 ± 2.5 nM Fe mg SRFA^{-1} found in Mediterranean seawater by Dulaquais et al. (2018) using a similar SRFA standard but a different analytical method (Pernet-Coudrier et al., 2013). The much lower ratio for the TAC method coincides with an underestimation relative to SA of the TPD Fe-binding ligand pool which is so strongly influenced by HS. However a very significant increase of 61 % (SD = 12.9, N = 47) of the $[L_t]_{SA}$ is still observed in $[L_t]_{TAC}$ with a strong correlation

with the TPD influence, as well as a positive increment ratio with [HS] of 68% the values for DFe and $[L_t]_{SA}$.

It may well be that the SRFA standard is too specific to describe fulvic acids as a group but it is the best we have presently as extensively explained by Sukekava et al. (2018). Furthermore, the Arctic today is subject to rapid loss of permafrost, releasing many complex organics into the rivers (Frey and McClelland, 2009), a signal already proven to reach well into the shelf seas (Vonk et al., 2012), adding to the (C)DOM pool transported by the TPD. The binding capacity of HS can very well have spatial and temporal differences that are currently not taken into account. Without the availability of HS standards that are specific for seawater, results need to be viewed in context of the standard used.

A near 1:1 ratio as found for $[L_t]_{HS}$ vs. $[L_t]_{TAC}$ inside the TPD (Figure 5B) can be interpreted as an indication that all Fe-binding organic ligands inside the TPD are HS, whereas Fe-binding organic ligands outside the TPD are of a different origin. These can be resulting from sea ice melt or of a marine origin, even marine humics. $[L_t]_{HS}$ vs. $[L_t]_{SA}$ gives an almost similar slope (0.89), but there is a strong offset compared to $[L_t]_{HS}$ vs. $[L_t]_{TAC}$ (Figure 5B). This indicates that using SA, Fe-binding organic ligands present outside the TPD are measured which are not measured using TAC. $[L_t]_{TAC}$ does not vary with $[L_t]_{SA}$ outside the TPD (Figure 4), more or less constant $[L_t]_{TAC}$ is also observed in relation to $[L_t]_{HS}$ (Figure 5B). This further indicates measurements with TAC do not represent all HS. Values for $[L_t]_{HS} > \delta L_t$ especially inside the TPD (Table 1, Figure 5C) could indicate that not all unrepresented HS are accounted for by measurements using SA as well. However, given the range of conversion factors reported (Laglera and van den Berg, 2009; Sukekava et al., 2018), this relation may depend on the conversion factor used. Additionally, δL_t combines two CLE-AdCSV measurements each with their own issues. The poor correlation between $[L_t]_{HS}$ and δL_t may further illustrate this (Table 3).

Given the limited resolution provided by the remarkably stable K´ values for either method, further characterization with CLE-AdCSV based measurements proves difficult. Correlation of $[L_t]_{HS}$ and $[L_t]_{TAC}$ is not significant outside the TPD, and the other correlation scores of $[L_t]_{HS}$ and CLE-AdCSV-derived $[L_t]$ are of poor significance (Table 3). There is no significant correlation or poor correlation between $[L_t]_{HS}$ and δL_t inside and outside of the TPD (Figure 5C) as shown by the constant ratio $[L_t]_{TAC}/[L_t]_{SA}$ irrespective of the TPD (Table 1). This suggests that the difference between the methods is not caused by the presence of HS in the TPD alone, and is indicative of a systemic difference between the CLE-AdCSV methods.

It has been shown that HS are resolved by the SA method of CLE-AdCSV (Abualhaija and van den Berg, 2014; Mahmood et al., 2015). Earlier work indicated that CLE-AdCSV using SA would be more suitable to detect weaker binding HS, whereas TAC is the stronger added ligand and therefore less able to establish a competitive equilibrium with HS (Laglera et al., 2011; Gledhill and Buck, 2012). Direct addition of the SRFA standard to a TAC-analysed sample did not result in any change in $[L_t]_{TAC}$ (Laglera et al., 2011; Chapter 5). TAC itself may interact with HS, which limits formation of the $FeTAC_2$ complex and obfuscates its competition with Fe-binding organic ligands in the sample (Laglera et al., 2011). Furthermore, where a stark difference is observed across the TPD influence, $logK'_{Fe'L}$ does not reflect this (Table 1). However, this is true for both TAC and SA methods in this study. From the present data it cannot be concluded whether TAC misses a specific ligand group or that a threshold value exist below TAC cannot detect HS because of an interference between TAC and HS as suggested by Laglera et al. (2011). Attributing the greater Fe-binding organic ligand concentrations found by the SA method to the ability of resolving the iron binding properties of HS alone is proven wrong here, as the representation of the Fe-binding organic ligand pool by either method is more nuanced. For one, increases in $[L_t]_{TAC}$ are observed in the humic-rich Arctic surface samples. While lower than $[L_t]_{SA}$, the increase in $[L_t]_{TAC}$ strongly correlates with HS descriptors (Chapter 5) and direct voltammetric measurements of HS with SRFA as a humic representative standard (Dulaquais et al., 2018; this study). While ligand saturation is found using the TAC method, suggesting part of the ligand pool is not measured, we do show that TAC sees at least part of the HS. TAC has been used successfully to relate HS to Fe-binding organic ligand concentrations on several occasions (Batchelli et al., 2010; Slagter et al., 2017; Dulaquais et al., 2018). However, this work calls into question if the entire contribution of HS to the complexing capacities reported was accounted for in those previous works. Uncertainties are exacerbated by the fact that $FeSA_2$ has been described as non-electroactive (Abualhaija and van den Berg, 2014). The equilibration time of 15 minutes is further influencing the results.

6.5. Conclusions

Analyses with SA as a competitive ligand were performed on select samples coinciding with analyses using TAC in Chapter 5. Additionally measurements of [HS] were performed as well. $[L_t]_{SA}$ was higher overall, but especially inside the TPD and explained the existence of high DFe above the solubility product of inorganic Fe-oxy(hydr)oxides. Still both CLE-AdCSV methods clearly show correlation with this TPD influence, which in turn is well-described by HS

properties including a representative $[L_t]_{HS}$ derived from the binding capacity of the SRFA standard used.

Both CLE-AdCSV methods have a ratio near 1 with $[L_t]_{HS}$, with an offset to higher concentrations for $[L_t]_{SA}$. While an $[L_t]_{HS}/[L_t]_{TAC}$ ratio near 1 could be seen as suggestive of domination of the Fe-binding organic ligand pool by HS, the occurrence of ligand saturation in TAC measurements, which is thermodynamically improbable, indicates that part of the (humic) ligand pool remains veiled using the TAC method. The offset between both methods does remain outside the TPD, but decreases. Here $[L_t]_{SA}$ decrease with $[L_t]_{HS}$, whereas $[L_t]_{TAC}$ does not, possibly due to a different origin of the (humic) ligands. Additionally, our results and the lack of response of CLE-AdCSV using TAC to addition of the SRFA standard in prior work further confirms that TAC cannot resolve part of HS.

Differences in $[L_t]$ using either method and correlations to HS are not reflected in K´, making it very difficult to recognize the contribution of HS by ligand class. Analysis using SA can be resolved for 2 ligand groups for more samples, again especially for surface samples. In these cases $logK_1´_{Fe´L(SA)}$ agrees reasonably with $logK_1´_{Fe´L(TAC)}$, and therefore presumably describe the same ligand group. $LogK_2´_{Fe´L(SA)}$ is weaker than $logK_2´_{Fe´L(TAC)}$, indicating a disparity in the ligands.

The HS carried across the Arctic Ocean surface by the TPD is responsible for the transport of DFe. Issues with TAC's ability to resolve certain HS lead to TAC only reflecting 61% of $[L_t]_{SA}$. Issues with SA equilibration may lead to an overestimation of $[L_t]$. In conclusion, comparison between methods brings a more complex relation to light, and suggests that method intercalibration in the presence of a variety of model ligands, multiple methods and detection windows may be required to properly ascertain the overall organic Fe-binding organic ligand pool in natural seawater samples. Especially in an area subject to complex changing terrestrial influences such as the Arctic Ocean.

Figure S1 (page 138)
Graphs representing from left to right: total ligand concentration ($[L_t]$), conditional binding strength ($logK'_{Fe'L}$), reactivity ($log\alpha_{Fe'L}$) and excess ligands (L'), for stations 69, 99,101,125 and 153 (rows of graphs). Shown are the top 200 m of the water column, with off scale plot lines indicating the next deeper value beyond. Closed symbols represent measurements with TAC, open symbols represent measurements with SA.